Spinodal Dewetting in Liquid Crystal and Liquid Metal Films

Stephan Herminghaus,* Karin Jacobs, Klaus Mecke, Jörg Bischof, Andreas Fery, Mohammed Ibn-Elhaj, Stefan Schlagowski

Theory predicts that dewetting of a homogeneous liquid film from a solid surface may proceed via unstable surface waves on the liquid. This phenomenon, usually termed spinodal dewetting, has been sought after in many systems. Observations in liquid crystal and liquid metal films showed that, as expected, the emerging structures were similar to those found for spinodal decomposition in mixtures. Certain differences, however, could be attributed to peculiarities of the wetting forces in these two dissimilar systems, thereby demonstrating the role of nonlinearities inherent in the wetting forces.

Structure formation in dewetting processes of thin liquid films has attracted much attention in recent years (*1–7*), in part because of the fundamental interest in basic interactions involved in wetting phenomena, but also because of the enormous technological relevance of adhesion failure mechanisms of coatings. Many unanswered questions still remain; in particular, the theoretically predicted scenario of spinodal dewetting, which proceeds via dynamically unstable surface waves, has proved difficult to observe experimentally. Here we report observations of spinodal dewetting in thin liquid crystal and liquid metal films from solid substrates. Direct comparison of the structures emerging in these two rather different systems not only yields insight into the relevant interactions, but also demonstrates the impact of the nonlinearities of the wetting forces on the dewetting process.

If the long-range forces across a wetting layer, such as the van der Waals force (*8*), are in favor of wetting, they act as the principal restoring forces of lateral film thickness fluctuations, that is, of thermally activated surface waves. Their amplitude is usually small relative to the film thickness, such that thermally activated nucleation of dry patches can be safely neglected. However, if the long-range forces do not favor wetting, they represent a driving force for thickness fluctuations, whose amplitude is thus expected to grow exponentially in time. In the valleys of these fluctuations, the liquid surface finally reaches the substrate and initiates dewetting (*9–11*).

S. Herminghaus, K. Jacobs, A. Fery, M. Ibn-Elhaj, S. Schlagowski, Max Planck Institute for Colloid and Interface Science, Rudower Chaussee 5, D-12489 Berlin-Adlershof, Germany. K. Mecke, Physics Faculty of the University of Wuppertal, D-42097 Wuppertal, Germany. J. Bischof, Faculty of Physics of the University of Konstanz, Post Office Box 5560, D-78434 Konstanz, Germany.

*To whom correspondence should be addressed. E-mail: herminghaus@mpikg.fta-berlin.de

The conditions for this to occur can be expressed in terms of the effective interaction potential of the film, $\Phi(h)$, which describes the interaction of the solid-liquid interface with the liquid-air interface (*12, 13*). $\Phi(h)$ may be defined as the excess free energy necessary to approach these two interfaces from infinity to the film thickness, h. For dewetting to occur, the global minimum of Φ must be at finite h, which then represents the equilibrium film thickness (Fig. 1A). It is readily shown (*9–11*) that if the second derivative of Φ with respect to h is negative, $\Phi''(h) < 0$, unstable modes exist whose amplitude grows exponentially according to $\exp(t/\tau)$, where τ is the growth time that is characteristic of the respective mode and depends on the wave number, q, of the mode (Fig. 1B). Furthermore, there is a characteristic wave number, q_m, for which τ^{-1} attains a maximum. The corresponding mode grows the fastest and is thus expected to dominate the emerging dewetting structure.

This process is analogous to spinodal decomposition, which can take place in mixtures if the second derivative of the free energy with respect to the composition, c, is negative, $\Phi''(c) < 0$ (*14, 15*). There as well, a certain mode with a characteristic wavelength is connected to the largest growth rate, τ^{-1}. By analogy, dewetting via unstable surface waves ($\Phi'' < 0$) has been termed spinodal dewetting. Although it is well known that in the case of spinodal decomposition the characteristic wavelength does indeed dominate the emerging structure, only a few analogous observations have been made in dewetting processes (*7, 16*), and there is currently no obvious explanation why the structures expected for a spinodal process are so scarcely observed in dewetting. In particular, the role of the substantial nonlinearity of the wetting forces and its possible impact on the emerging structures has not yet been investigated experimentally. Consequently, we have studied the dewetting behavior of two rather different systems showing spinodal dewetting (namely, liquid crystal and liquid metal films) in an effort to elucidate some aspects of the interplay of nonlinearity and dewetting morphology.

To study the dewetting of liquid crystal (LC) films, we used thin films of tris(trimethylsiloxy)silane-ethoxycyanobiphenyl ($5AB_4$) (*17*). This material undergoes a phase transition from the crystalline to the isotropic state at 18°C. Films of $5AB_4$ were prepared by spreading the material from chloroform solution onto the surface of deionized water in a Langmuir trough at 10°C. By surface compression, films with a typical thickness of $h = 40$ nm could easily be formed (*17*). The films were transferred at a surface pressure of 6.9 mN m^{-1} onto silicon wafers that had been cleaned and hydrophilized by a modified "RCA procedure" (*18*). Because $5AB_4$ is a (soft) solid at 10°C, the films break into patches upon transfer, typically several hundred micrometers in size.

The LC film dewets in the course of several minutes through various dewetting mechanisms. Circular "dry" holes appear, the rim of which is formed by the material removed from the hole (Fig. 2A). This is a result of nucleation from defects in the film, as discussed above. In addition, dewetting by an undulative mode occurs across the patch, which exhibits a clearly defined critical wavelength, as expected for spinodal dewetting. Light microscope observation of the dewetting process shows that the nucleated dewetting begins almost immediately and proceeds gradually with time. In contrast, the undulative mode is not visible at first, but appears after some time (several seconds to minutes), then grows rapidly in amplitude until it reaches the "final" state shown in Fig. 2. This is the behavior expected for a dynamically unstable mode.

The spinodal dewetting in this system may be qualitatively understood from the molecular interactions. The LC molecules are strongly dipolar, and thus a strongly polar substrate is required for the preparation of homogeneous films (complete wetting); otherwise there would be dewetting by the strong cohesion resulting from the long-range dipolar forces. It is therefore not surprising that thick films can be generated on the Langmuir trough, given the high relative permittivity ($\varepsilon \approx 80$) of the underlying water (*19*). In contrast, when the film is transferred onto the silicon wafer, the substrate polarizability is decreased by a factor of ~20, thus reducing the polar adhesion to the substrate considerably and rendering the long-range tail of $\Phi(h)$ negative. We interpret this as being the cause of the observed dynamical instability of the surface ripples, which leads to the characteristic dewetting pattern (Fig. 2A).

The presence of this undulation, which appears at first glance as a dewetting pattern close to equilibrium (*20*), does not inhibit the

growth of the circular holes nor the recession of the edge of the patch. The reason for this behavior can be seen by imaging the LC profile with the use of scanning force microscopy (SFM), which provides the resolution necessary to resolve its fine structure (*21*). The data in Fig. 2B show that dewetting leaves a smectic trilayer (arrow), which seems to represent the global minimum of the effective interaction potential for this system. Farther to the left, two periods of the undulation structure are visible. The minima of the undulation, which had at that point already reached a configuration steady enough for SFM, do not represent the trilayer thickness but instead a much larger thickness of ~28 nm. This thickness seems to represent a local (metastable) minimum of the effective interaction potential (*22*).

Quantitative information about $\Phi(h)$ can be obtained from the undulation wavelength and the contact angle at the trilayer. Assuming that $\Phi(h) \propto h^{-2}$ for large thicknesses, as expected for dispersive as well as dipolar interactions, we can construct most of the properties of $\Phi(h)$ (Fig. 2C). The requirement of a local minimum at 28 nm enforces a large difference in energy between the local and the global minimum. This is in accordance with the above observations. The energy scale is comparable to the interaction energy of the molecular dipoles [≈6 D (*17*)] with their images in a highly polar medium such as water. This corroborates the above conjecture that withdrawal of the water subphase may initiate spinodal dewetting. Spatial director correlations in the LC may attain a range of several nanometers, even far from the phase transition temperature (*23, 24*), and thus may give rise to the observed local minimum in $\Phi(h)$. The precise nature of this effect, however, remains to be clarified.

The presence of the local minimum in $\Phi(h)$, which leads to the saturation of the undulation at rather small amplitudes, renders the system analogous to spinodal decomposition in a mildly quenched mixture, where the stable concentration corresponding to the coexistence curve (or the "binodal line") represents a similar stabilizing shallow minimum in the free energy. In our system, the local minimum in $\Phi(h)$ precludes the strong nonlinearity of the dispersion forces, which diverge close to the surface, from coming into play. In contrast, in the absence of a stabilizing force such as the one encountered here, the inherent nonlinearity of the dispersion forces may have a visible impact on the dewetting morphology. By nonlinearity, we mean that when the film surface approaches the substrate interface, the driving force $\Phi(h)$ is no longer constant (as for small undulation amplitudes) but varies strongly, such that the system cannot be described by linear differential equations.

To study the effect of nonlinearity, we have investigated spinodal dewetting in liquid metal films. Metals are expected to show spinodal dewetting from moderately polarizable substrates, such as quartz glass (*25, 26*), because of their high polarizability. However, no intermediate-range stabilizing forces such as those in the LC are to be expected. Thus, liquid metal films should be good model systems for studying inherent nonlinear effects in spinodal dewetting.

Metal films (Au, Cu, and Ni) with thicknesses ranging from 25 to 50 nm were thermally evaporated onto fused silica substrates (*27*), and dewetting was induced by melting the solid film. Because the viscosity of liquid metals is orders of magnitude lower and the surface energies are much higher than for LC materials (*28*), dewetting takes place on a sub-microsecond time scale. For this reason, melting was induced by irradiation with a frequency-doubled, Q-switched Nd–yttrium-aluminum-garnet (Nd:YAG) laser pulse (λ = 532 nm; pulse duration, 7 ns). As is well known, irradiation with energies in the range of a few hundred millijoules per square centimeter leads to melting of the metal film for a well-defined period of time, the duration of which is a monotonically increasing function of laser fluence (*16*). The solidified film thus represents a snapshot of the film structure at the instant of resolidifica-

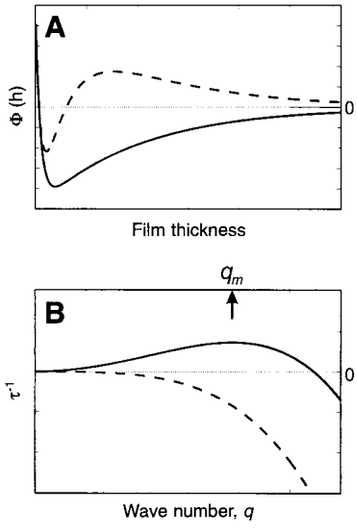

Fig. 1. (**A**) Sketch of $\Phi(h)$ corresponding to incomplete wetting (global minimum at finite h) but with the long-range forces in favor (dashed line) or in disfavor (solid line) of wetting. By "long range" we denote the region well to the right of the maximum of the dashed curve of $\Phi(h)$. (**B**) The growth rate versus the wave number, q, of the mode, plotted for the two cases $\Phi''(h_0) > 0$ (dashed line) and $\Phi''(h_0) < 0$ (solid line). In the latter case, there are unstable modes, which span the range from $q = 0$ up to the zero of $\tau^{-1}(q)$. The mode that grows the fastest is characterized by the wave number q_m, which represents the maximum of $\tau^{-1}(q)$.

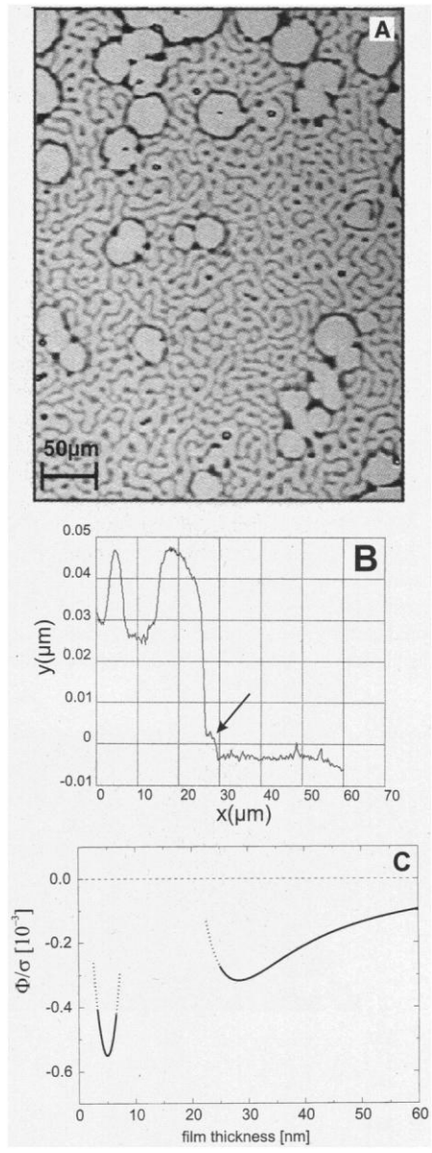

Fig. 2. (**A**) Reflection micrograph of a patch of $5AB_4$ at room temperature, after transfer from the Langmuir trough to a silicon wafer. Circular holes nucleated from defects are clearly distinguished, as is an undulative mode indicating spinodal dewetting. (**B**) Topography of $5AB_4$ dewetting structure, as obtained by SFM, close to the edge of a dewetted patch. The x- and y-axes are the horizontal and vertical length scales of the topography, respectively. Clearly visible are the undulation (to the left) as well as a 5-nm-thick bottom layer (arrow). The latter is identified with the stable trilayer, which is known to be particularly stable for this system (*17*). The slope to the higher elevation, to the left of this step, represents the receding edge of the liquid. (**C**) $\Phi(h)$ for the LC film in units of the (unknown) surface tension σ of the liquid crystal, as inferred from the morphology of the dewetting pattern. The requirement of a local minimum at 28 nm entails a large energy difference between the local and the global minimum. This explains the ability of the circular holes to keep growing even in a fully developed undulation structure.

tion. Ex situ characterization of the film topography was carried out by optical microscopy and SFM.

In an optical transmission micrograph of an irradiated gold film (Fig. 3A), the melt duration decreases from left to right because of the slight lateral variation of the laser fluence (Gaussian beam profile). To the left, the fluence was sufficient to remove the film, but on the remainder of the displayed area, evaporation of material could be safely neglected (*16*). Analogous to the observations on the LC films, two different dewetting modes can be identified clearly. Heterogeneously nucleated circular holes are randomly distributed over the sample. Their appearance agrees with what has been observed in other systems (*1, 4–6*). In addition, a second dewetting structure is readily recognized as the result of unstable surface waves on the film. Undulations are visible in the center of the image as spots of slightly enhanced brightness, with a certain preferred distance (*6*). This distance scales with the film thickness in the way predicted by the theory of spinodal dewetting, as has already been shown (*16*). Farther to the left, we see the fully developed dewetting morphology, the appearance of which is, at least at first glance, similar to that in the LC films (Fig. 2A).

The fact that the heterogeneously nucleated holes grow linearly with time (*29*) can be exploited by using them as a clock for the dewetting process. Each hole provides, by its diameter, a data point for the melt duration in its immediate environment (Fig. 3B). Obviously, the dewetting process is completed within a short period relative to the total melt duration, as expected for an exponentially growing mode amplitude.

Closer inspection reveals that there are marked differences with respect to Fig. 2. In the "transition region" between the closed film and the dewetted area, it can be seen that dewetting proceeds by the formation of single holes (white arrows), each corresponding to a valley of the undulation. In contrast, on-line inspection of the undulation buildup in the LC films revealed a continuously growing amplitude of a rather smooth undulation, with no individual holes forming. To analyze this in more detail, we adjusted the laser system to yield a large region of very homogeneous laser fluence. In this way, we could prepare samples with an extended transition region in which an undulation and a large number of holes formed from undulation valleys were present (Fig. 4).

Figure 4A shows a SFM image of a small part of such a sample. A number of holes with similar sizes are present, whereas the undulation can be only faintly seen on that scale. In Fig. 4B, which shows the topographic cross section indicated in Fig. 4A, the slopes of the holes become progressively steeper toward the minima of the film thickness or, even more, toward the contact line with the

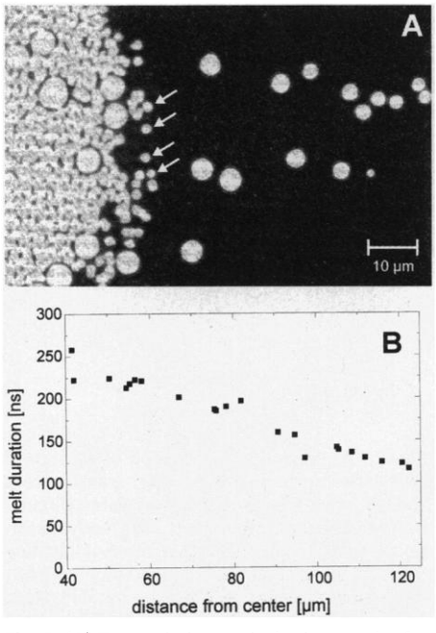

Fig. 3. (**A**) Transmission optical micrograph of a gold film after irradiation with a Q-switched Nd:YAG laser pulse. Similar to the liquid crystal, two dewetting modes can be clearly distinguished, one of which points to the presence of unstable surface waves. In the transition region between the closed film (right) and the fully dewetted film (left), dewetting from the valleys of the undulation proceeds via the formation of single holes (white arrows). (**B**) Melt duration, as inferred from the diameters of the holes, plotted as a function of distance from the center of the laser spot. The time axis was gauged by simultaneous measurements of the melt duration by optical reflectometry (*16*). The horizontal axis covers the whole range corresponding to (A).

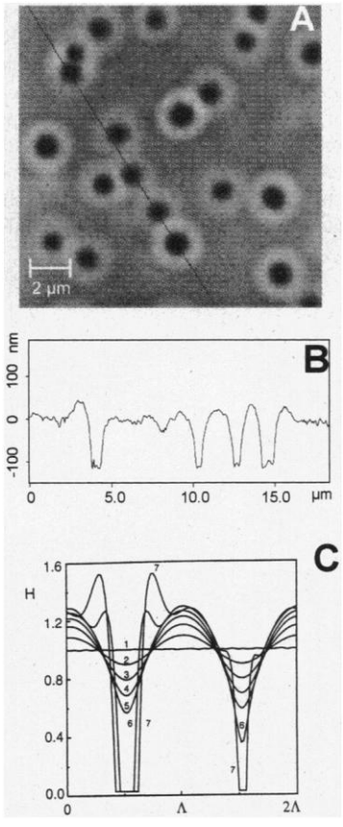

Fig. 4. (**A**) Topography of the intermediate state of dewetting of a gold film (obtained with SFM). At this scale, the undulation is only faintly visible. The topographic section (**B**) is remarkably similar to recently published results of a simulation of the fully nonlinear spinodal dewetting problem (*30*) (**C**), where H and Λ are the nondimensional thickness and lateral length, respectively, normalized by characteristic scales of the system. The numbers 1 to 7 indicate the time evolution of the simulation, corresponding to a nondimensional time scale of T = 0.0001, 21.05, 23.4, 24.41, 24.9, 25.25, and 25.3, respectively.

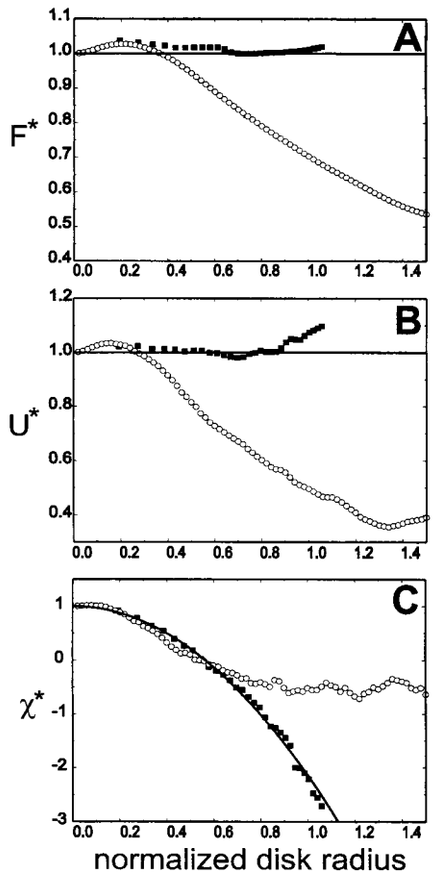

Fig. 5. Integral geometry analysis of hole distributions found in dewetting by heterogeneous nucleation (polymer film) and spinodal dewetting (metal film). Data are displayed for holes in a polystyrene film (*6*) (■) and for holes in the gold film as in Fig. 4A (○); the solid lines represent the prediction for a purely random ensemble. The Minkowski measures displayed are (**A**) the normalized total area F^* of the set, (**B**) its normalized boundary length U^*, and (**C**) its Euler characteristic χ^*.

substrate. This compares favorably with what would be expected as a result of the strong nonlinearity of the van der Waals potential, as can be seen by comparison with the simulation in Fig. 4C (*30*). The qualitative agreement is obvious.

An interesting question as to the spatial distribution of the holes arises from Fig. 4. At this stage of dewetting, the distribution appears to be quite random, similar to what is observed in the standard rupture scenario of polymer films (*6*). Does the correlation of the valley positions manifest itself noticeably in correlations of the hole positions, such that it is possible to distinguish the mechanism simply by analysis of their spatial distribution? The two-point correlation function of the hole positions does not reveal a significant difference between the spatial distribution of the holes in the gold film and those nucleated heterogeneously in a polymer film (*6*). However, by using the more elegant method of the so-called Minkowski measures, a clearer distinction becomes possible. Let us consider the centers of the holes in a film as an ensemble of points in the plane. On each point, let us put a circular disk, each with the same radius r, with its center on that point. Now let us consider the set defined as the set union of all disks. This is a complicated object whose geometrical properties depend on r. It is now useful to consider the morphological Minkowski measures of this object: its area, its boundary length, and its Euler characteristic (Fig. 5) (*31*). It turns out that these quantities, which are readily evaluated on a computer, are very sensitive to spatial correlations in the distribution of the initial ensemble of points.

In Fig. 5, we plotted these three quantities as a function of the disk radius, r. They are represented in a normalized form, such that the functional dependences for a purely random ensemble become simple. Aside from certain deviations in the boundary length (U^*), which can be attributed to the finiteness of the ensemble, the holes in the polymer film show good agreement with the predicted values for a purely random ensemble. In contrast, the data obtained with the gold film show substantial deviations. These data can be construed as confirming that the holes observed in the gold film are not generated by a random process such as heterogeneous nucleation, as the correlations in the hole positions are clearly visible by the strong deviation from the solid lines. They have formed instead from the valleys of the unstable undulation, which provides the observed correlation. However, the presence of the correlation in the spatial distribution of the hole positions demonstrates, in turn, that even though the appearance of the ensemble of holes may seem random at first glance, it inherited the specific correlations imposed by the spinodal process and may be identified by suitable methods such as the Minkowski measures.

References and Notes

1. G. Reiter, *Phys. Rev. Lett.* **68**, 75 (1992).
2. A. Sharma and A. T. Jameel, *J. Colloid Interface Sci.* **161**, 190 (1993).
3. M. Elbaum and S. G. Lipson, *Phys. Rev. Lett.* **72**, 3562 (1994).
4. G. Henn, D. G. Bucknall, M. Stamm, P. Vanhoorne, R. Jerome, *Macromolecules* **29**, 4305 (1996).
5. T. G. Stange, D. F. Evans, W. A. Hendrickson, *Langmuir* **13**, 4459 (1997).
6. K. Jacobs, S. Herminghaus, K. R. Mecke, *ibid.* **14**, 965 (1998).
7. R. Xie, A. Karim, J. F. Douglas, C. C. Han, R. A. Weiss, *Phys. Rev. Lett.* **81**, 1251 (1998).
8. We discuss only films with a thickness within the range of the dispersion forces, that is, not thicker than ~100 nm.
9. A. Vrij, *Discuss. Faraday Soc.* **42**, 23 (1966).
10. E. Ruckenstein and R. K. Jain, *Faraday Trans. II* **70**, 132 (1974).
11. F. Brochard-Wyart and J. Daillant, *Can. J. Phys.* **68**, 1084 (1990).
12. S. Dietrich, in *Phase Transitions and Critical Phenomena*, C. Domb and J. L. Lebowitz, Eds. (Academic Press, London, 1988), vol. 12, pp. 1–218.
13. M. Schick, in *Les Houches Session XLVIII, 1988: Liquids at Interfaces*, J. Charvolin *et al.*, Eds. (Elsevier Science, Amsterdam, 1989), pp. 415–497.
14. J. W. Cahn, *J. Chem. Phys.* **42**, 93 (1965).
15. V. S. Mitlin, *J. Colloid Interface Sci.* **156**, 491 (1993).
16. J. Bischof, D. Scherer, S. Herminghaus, P. Leiderer, *Phys. Rev. Lett.* **77**, 1536 (1996).
17. M. Ibn-Elhaj, H. Möhwald, M. Z. Cherkaoui, R. Zniber, *Langmuir* **14**, 504 (1998).
18. R. Riegler and M. Engel, *Ber. Bunsenges. Phys. Chem.* **95**, 1424 (1991).
19. The influence of the dipolar polarizability of the subphase on long-range wetting forces has been shown in studies on the wetting of pentane on water [K. Ragil, J. Meunier, D. Broseta, J. Indekeu, D. Bonn, *Phys. Rev. Lett.* **77**, 1532 (1996)], among others.
20. Ripening of these structures was too slow to be observed on experimental time scales.
21. The possibility of imaging polar liquids has recently been demonstrated [A. Fery and S. Herminghaus, *Ultramicroscopy* **69**, 211 (1997)].
22. The system thus relaxes toward a film of finite thickness, that is, incomplete wetting. This justifies the well-established term "dewetting," even though the process does not leave a perfectly dry surface.
23. B. M. Ocko, A. Braslau, P. S. Pershan, J. Als-Nielsen, M. Deutsch, *Phys. Rev. Lett.* **57**, 94 (1986).
24. P.-G. DeGennes, *Langmuir* **6**, 1448 (1990).
25. M. J. Godbole, A. J. Pedraza, D. H. Lowndes, J. R. Thompson, *Mater. Res. Soc. Symp. Proc.* **235**, 583 (1992).
26. D. J. Srolovitz and M. G. Goldiner, *J. Met.* **3**, 31 (1995).
27. An intermediate layer of a few monolayers of chromium (thickness <2 nm) was deposited to improve the adhesion of the films.
28. T. Iida and R. I. L. Guthrie, *The Physical Properties of Liquid Metals* (Oxford Univ. Press, Oxford, 1987).
29. For simple monatomic liquids such as gold, the liquid is not expected to slip along the substrate. In the absence of slippage, the holes grow linear with time [F. Brochard, P. G. DeGennes, H. Hervert, C. Redon, *Langmuir* **10**, 1566 (1994)].
30. R. Khanna and A. Sharma, *J. Colloid Interface Sci.* **195**, 42 (1997).
31. K. R. Mecke, T. Buchert, H. Wagner, *Astron. Astrophys.* **288**, 697 (1994).

32. Stimulating discussions with G. Reiter, A. Sharma, and P. Leiderer are gratefully acknowledged.

29 June 1998; accepted 15 September 1998

Control of Chemical Reactions by Feedback-Optimized Phase-Shaped Femtosecond Laser Pulses

A. Assion, T. Baumert,* M. Bergt, T. Brixner, B. Kiefer, V. Seyfried, M. Strehle, G. Gerber

Tailored femtosecond laser pulses from a computer-controlled pulse shaper were used to optimize the branching ratios of different organometallic photodissociation reaction channels. The optimization procedure is based on the feedback from reaction product quantities in a learning evolutionary algorithm that iteratively improves the phase of the applied femtosecond laser pulse. In the case of $CpFe(CO)_2Cl$, it is shown that two different bond-cleaving reactions can be selected, resulting in chemically different products. At least in this case, the method works automatically and finds optimal solutions without previous knowledge of the molecular system and the experimental environment.

When lasers were invented they were considered the ideal tool for microscopic control of chemical reactions, that is, selective cleavage or formation of chemical bonds (*1*, *2*). By exactly tuning the monochromatic laser light according to the local mode frequency of a specific chemical bond, it was thought that enough energy could be deposited in this specific mode to cause selective bond breakage (*3*). In most experiments, however, selectivity is lost because of rapid intramolecular energy redistribution (*1*). Several control schemes have been proposed that make use of the coherent nature of laser radiation. Known as "coherent control," these schemes access

Physikalisches Institut, Universität Würzburg, Am Hubland, 97074 Würzburg, Germany.

*Present address: Deutsches Zentrum für Luft- und Raumfahrt, 82230 Wessling, Germany.